Published in final edited form as:
*Cancer Res*. 2009 July 1; 69(13): 5505–5513. doi:10.1158/0008-5472.CAN-08-4311.

# Expression of WSX1 in tumors sensitizes IL27-signaling independent NK cell surveillance

**Denada Dibra**[1], **Jeffry J. Cutrera**[1], **Xueqing Xia**[1], **Mark P. Birkenbach**[2], and **Shulin Li**[1]

[1] Department of Comparative Biomedical Sciences, Louisiana State University, Skip Bertman Drive, Baton Rouge, LA 70803

[2] Department of Pathology, Temple University School of Medicine, 3401 N. Broad Street, Philadelphia, PA 19140

## Abstract

It is well known that the interleukin (IL) 27 receptor WSX1 is expressed in immune cells and induces an IL27-dependent immune response. Opposing this conventional dogma, this study reveals a much higher level of WSX1 expression in multiple types of epithelial tumor cells when compared to normal epithelial cells. Expression of exogenous WSX1 in epithelial tumor cells suppresses tumorigenecity *in vitro* and inhibits tumor growth *in vivo*. Different from the role of WSX1 in immune cells, the antitumor activity of WSX1 in epithelial tumor cells is independent of IL27 signaling but is mainly dependent on NK cell surveillance. Deficiency of either the IL27 subunit Epstein–Barr virus-induced gene 3 (EBI3) or the IL27 receptor WSX1 in the host animals had no effect on tumor growth inhibition induced by WSX1 expression in tumor cells. Expression of WSX1 in epithelial tumor cells enhances NK cell cytolytic activity against tumor cells, while the absence of functional NK cells impairs the WSX1-mediated inhibition of epithelial tumor growth. The underlying mechanism by which WSX1 expression in tumor cells enhances NK cytolytic activity is dependent on upregulation of NKG2D ligand expression. Our results reveal an IL27-independent function of WSX1—sensitizing NK cell-mediated antitumor surveillance via an NKG2D-dependent mechanism.

### Keywords

Innate Immunity; NK cell; IL27; Interleukin; TCCR; Tumor; WSX1

## Introduction

IL27 receptor WSX1 is most homologous to the IL12 receptor β2 chain (1). WSX1 together with gp130 constitute a functional signal-transducing receptor for IL27, whereas lack of either subunit attenuates IL27-mediated signaling (2). WSX1 is reported to be expressed in immune cells such as monocytes, dendritic cells, T and B lymphocytes, NK cells, mast cells, and endothelial cells (1).

In a patent application (PCT/2007/0280905), we reveal that WSX1 is detectable in breast epithelial tumor cells. This discovery is further supported by a recent report which revealed that WSX1 is expressed in another type of epithelial tumor, melanoma cells (3). The same as

Corresponding Author: Shulin Li, Paula and Milton W. Shepard Endowed Professor, Department of Comparative Biomedical Sciences, Louisiana State University, Skip Bertman Drive, Baton Rouge, LA 70803, e-mail: E-mail: sli@vetmed.lsu.edu, phone: 225-578-9035, Fax: 225-578-9895.

**Disclosure of Potential Conflicts of Interest:** No potential conflict of interest were disclosed

found in immune cells, WSX1 is functional in these epithelial tumors cells as indicated by the IL27-mediated activation of STAT1 and STAT3 (3).

Clearly, the reports found in the literature suggest that WSX1 plays a role through the IL27 signaling pathway, but the IL27-independent role of WSX1 in promotion or inhibition of tumorigenesis has not been reported yet. Using genetically modified tumor cells, we present evidence that the expression of WSX1 in epithelial tumor cells suppresses tumor growth both *in vitro* and *in vivo*. Such inhibition of tumor growth is dependent on NK cells but independent of IL27 signaling. Our results reveal a novel function of WSX1 in epithelial tumor cells, which is to sensitize NK-mediated antitumor immunosurveillance in an IL27-independent manner.

## Materials and Methods

### Cell culture and reagents

Human cancer cell lines from different tissue origins including Hela, HT29, HCT116 and 4T1 were purchased from ATCC. Human breast cancer cell lines MDA468, MDA231, and MCF7 were provided by Dr. Bolin Liu (University of Colorado Denver School of Medicine at Aurora, CO). The normal colon cell line NCM460 was purchased from INCELL Cooperation, LLC. UM-SCC11A, UM-SCC11B, UM-SCC17A, and UM-SCC17B are head and neck squamous cell carcinomas provided by Dr. Thomas Carey (University of Michigan, Ann Arbor, MI) (4). Mouse HPV-associated tumor cell line TC1 was provided by Dr. T. C. Wu (John Hopkins University, Baltimore, MD) (5). The mouse squamous cell carcinoma cell line AT84 was provided by Dr. Edward Shillitoe (State University of New York Upstate Medical School, Syracuse, NY). Recombinant mouse IL27, NKG2D/Fc, monoclonal anti-human WSX1, and anti-human MICA-Pe antibody were purchased from R&D Systems. Anti-mouse pSTAT1-701, anti-mouse IgG-PE, actin, anti-human IgG-PE, and anti-hamster IgG-PE were purchased from Santa Cruz Biotechnology. Anti-NKG2D C7 was provided by Dr. Wayne Yokoyama (Washington University School of Medicine, St. Louis, MO).

### Quantitative real-time PCR

Total RNA was isolated from cells using TRIzol Reagent (Invitrogen). Residual genomic DNA was removed from total RNA using the TURBO DNA-*free*™ kit (Applied Biosystems/ Ambion). Two micrograms of RNA were used for cDNA synthesis using the High Capacity RNA-to-cDNA Kit (Applied Biosystems). The relative gene expression levels were determined using quantitative Real-time PCR and SYBR green labeling method in an ABI 7300 Sequence Detector (Applied Biosystems). The reaction contained 2 μL of cDNA, 12.5 μL the SYBR Green PCR Master Mix (Applied Biosystems), and 200–250 nM of primer in a total volume of 25 μL. The PCR cycling conditions were as follows: 40 cycles of 15 s at 95°C, 60 s at 60° C. All samples were run in duplicates. PCR amplification of β-actin was performed using 0.1 μL of cDNA. The $C_T$ value of each sample was acquired, and the relative level of gene expression was calculated by the Delta $C_T$ method, which was normalized to the endogenous control of β-actin. Data were expressed as an n-fold relative to control. The forward and reverse primer sequences for the human β-actin and WSX1 detection are: 5′ AGAGGGAAATCGTGCGTGAC3′ and 5′CAATAGTGATGACCTGGCCGT3′, respectively. WSX1: 5′GAGCCCCCTCCGAGTTACAC3′ (forward) and 5′ AGCTGTTCCCGAGGAATGG3′ (reverse).

### Establishing stable WSX1 expressing cell lines

The murine WSX1 gene was purchased from Open Biosystems and subcloned into pBMN-GFP plasmid (Phoenix™ Retrovirus Expression System, Orbigen, Inc.). The retrovirus was produced by transfecting mWSX1/GFP constructs into Phoenix eco packaging cells. AT84 and TC1 cells were infected with retroviral containing supernatant derived from the transduced

HEK293 cells. The transduction was confirmed by detecting green fluorescent protein (GFP) expressing cells under the fluorescence microscope. Cell colonies with GFP expression from a single cell were picked, expanded, and further confirmed for WSX1 expression using Flow Cytometry. Using this approach, both WSX1/GFP and GFP positive TC1 and AT84 cells were obtained.

### Animal procedures

All the animal procedures were approved by the IACUC at Louisiana State University. Six- to eight-week-old mice were used for this study. The subcutaneous tumor models were generated by subcutaneously inoculating TC1 and AT84 tumor cells ($2\times10^5$ in a 30-μL volume per mouse) into mice. Tumor measurement and calculation were the same as described previously (6). C57Bl/6 WSX1 knockout mice were provided by Dr. Fred de Sauvage (Genentech), and C57Bl/6 EBI3 knockout mice were provided by Dr. Mark P. Birkenbach (Temple University School of Medicine, Philadelphia, PA). C57Bl/6, Balb/c SCID, C3H, C57Bl/6 perforin, and Rag deficient mice were purchased from commercial sources.

### NK cytotoxicity assay

NK cell activity was evaluated using the CyToxiLux kit (OncoImmunin,Inc.), a single-cell-based fluorogenic cytotoxicity assay (7,8). Effector cells were prepared from spleens as previously described (8) and incubated with red fluorescence-labeled target cells at a ratio 100:1, 50:1, and 25:1 in 200 μL cell culture media. Target cells alone were used as control for spontaneous cell death. Sixteen hours after incubation, adhesive target cells were washed with PBS. Alive red target cells (input target cells) were counted using Olympus BX41 fluorescence microscope. NK activity was calculated using the following equation: % NK cell activity = 100 × (input target cells – output target cells)/(input target cells).

### Flow Cytometry

Cells were stained with the indicated primary and secondary antibodies for 30 min at 4° as indicated in each figure. The expression of the indicated genes was analyzed on FACS Calibur and Cellquest graphics software (BD Biosciences).

### Cell proliferation

Cell proliferation assays were performed using the luminescence ATP Lite assay detection system (PerkinElmer). Briefly, 500 cells were seeded in a 96 well plate; cells were lysed on days 0, 2, and 4 for measuring the ATP levels. The cell proliferation index was calculated using the following equation: Cell proliferation index= [ln (d)]/[ln (d0)], where ln (d) = natural log at the day when cells were lysed; ln (d0) = natural log at the day when cells were seeded.

### Soft agar growth assay

The clonogenic assay was performed as previously described (9). Briefly, genetically engineered cells ($5\times10^3$ for TC1-GFP and TC1-WSX1 cells and $1\times10^3$ for AT84-GFP and AT84-WSX1 cells) were suspended in 0.34% agar in cell culture media (Sigma, St Louis, MO). The mixture solution was layered on solid agar support prepared from 0.9% agar in cell culture media. The cells were seeded in triplicates on a 6-well plate and grown for 2 weeks. Colonies were counted under a 10x dissecting microscope after staining with 0.05% Crystal Violet for 1 h. Images were captured using Molecular Image Gel Dox XR (Biorad).

### Western blot

Cells ($5\times10^5$), growing in 10% heat-inactivated FBS-containing culture media, were treated with or without IL27 (20 ng/mL) for the indicated times. Protein extract was obtained by

directly lysing cells using 60 μL of Laemmli sample buffer. Twenty microliters of total protein extract from each sample were separated by SDS-PAGE, transferred to a nitrocellulose membrane and incubated with primary antibody overnight at 4° C (750x dilution for anti-pSTAT1/701 and 1000x fold dilution for anti-Actin).

### Statistical analysis

For *in vivo* experiments, Univariate Repeated Measures ANOVA was used to analyze the difference among treatments using SAS version 9.1.3. When appropriate, Tukey's HSD test was performed for interaction affects. For *in vitro* results, student's T test analysis was conducted.

## Results

### A much higher level of functional WSX1 is expressed in most of the tested epithelial tumor cells than in normal epithelial cells

It is well known that the IL27 receptor WSX1 is expressed mainly in immune cells and the only other type of cells expressing this gene is endothelial cells. However, recently we and others have found WSX1 expression in breast and melanoma epithelial tumor cells lines (3). To determine whether the WSX1 expression in epithelial tumor cells plays an important function, we have compared the magnitude of WSX1 expression between normal and tumor epithelial cells. The quantitative analysis result demonstrated that WSX1 was present not only in breast cells but also in colon, cervical, and squamous cell carcinoma tumor cells, suggesting that WSX1 was expressed in most human epithelial tumor cells (Fig. 1*A*). However, the expression level of this gene varied greatly among the different cell lines when compared to the normal epithelial cell line NCM460 (Fig. 1*A*). A few cell lines such as HT29 and UM-SCC17A showed 6.9–8.4-fold lower expression of WSX1 when compared to a normal epithelial cell line, NCM460, while most of the cell lines such as Hela, HCT116, and UM-SCC11A showed much higher levels of expression (ranging from 13–78 times higher than NCM460). The high level of WSX1 expression in most of the epithelial tumor cells but not in the normal epithelial cells suggests that WSX1 may play a role in regulating tumor progression. The level of WSX1 protein expression was positively associated with the level of mRNA (Fig. 1*B*).

Since WSX1 is the receptor of IL27, one obvious question is whether the high level of gene expression is associated with a high level of function. We used phosphorylation of STAT1 by IL27 as a functional WSX1 end point. After 10 min of incubation with IL27 (the second lane in each panel, Fig. 1*C*), IL27 induced phosphorylation of STAT1; such an increase correlates well with the presence of WSX1 expression but does not correlate with the absolute level of WSX1 expression (Fig. 1*B*). The human cell lines HT29 and UM-SCC17A lacking WSX1 expression showed very low to no detectable STAT1 phosphorylation, while cell lines such as Hela, HCT116, and UM-SCC11A with WSX1 expression showed an increase in phosphorylation of STAT1. However, a similar level of phosphorylation was detected in both the low (NCM460 and UM-SCC17B) and high (HCT116 and Hela) level WSX1-expressing cells (Fig. 1*C* vs. 1*A*).

### WSX1 reduces tumorigenecity and proliferation of epithelial tumor cells

The results from others exclusively illustrate that WSX1 plays a role in inducing an immune response through IL27-signaling in immune cells. The result from Fig. 1*B* confirms that the IL27/WSX1 signaling occurs in epithelial tumor cells. However, the high level of WSX1 expression does not correlate to the STAT1 phosphorylation in most epithelial tumor cells (Fig. 1*C*). Moreover, the endogenous IL27 is undetectable in either serum or splenocytes and, therefore, may not initiate any signaling in either tumor or host cells during tumorigenesis and

development. These facts suggest that a high level of WSX1 expression alone may affect tumorigenesis, which is the central hypothesis to be tested below.

To determine whether increased WSX1 expression alone may regulate IL27 signaling-independent tumor development, a clonogenic assay was performed to determine the tumorigenecity and proliferative ability of tumor cells engineered with WSX1 or GFP control genes. This method has been known to be effective in determining these end points (10). Flow cytometry analysis confirmed the expression of WSX1 in the stable transfected cell clones (Fig. 2*A*). The clonogenic assay results illustrated that expression of WSX1, but not GFP, dramatically reduced the ability of cells to grow in soft agar in both TC1 and AT84 cells (Fig. 2*B and 2C*).

To further confirm the inhibitory effect of WSX1 expression on tumor cells, cell proliferation was determined. Similar to the clonogenic assay, WSX1 significantly reduced the proliferation of TC1 and AT84 cells, but the inhibition of AT84 proliferation by WSX1 expression was at a much lower magnitude when compared to TC1 (Fig. 2*D*).

## WSX1 suppresses tumor growth *in vivo* in both TC1 and AT84 tumor models

Although the clonogenic assay is a good predictor of tumorigenecity *in vitro*, it does not read any host cell-induced cytotoxic end-points that occur in a true tissue environment (11). To avoid this problem, the effect of WSX1 expression on tumor growth was tested in syngeneic mice by subcutaneously inoculating with GFP or WSX1-expressing tumor cells. In agreement with the *in vitro* assay result, WSX1 expression almost completely abolished TC1 tumor growth (Fig. 3 A). Likewise, WSX1 expression also inhibited AT84 tumor growth in a different mouse strain (Fig. 3 B). The remarkable difference in the tumor growth rate shown in TC1 and confirmed in AT84 strongly indicates that WSX1 has a tumor suppressive role in epithelial tumor cells.

## WSX1-mediated suppression of tumor growth is dependent on NK cells

The direct antitumor mechanism by WSX1 was not found in the literature, but one possible explanation could be due to the reduction of tumor cell proliferation as observed *in vitro* (Fig. 2*D*). However, the dramatic difference in tumor growth *in vivo* (Fig. 3*A*) when compared to the small difference of proliferation *in vitro* (Fig. 2*D*) between TC1-WSX1 and TC1-GFP indicates that cell proliferation differences alone may not be the major cause for the diminished tumor growth in the presence of WSX1. An alternative assumption is that WSX1 expression in tumor cells may enhance the immune surveillance by the host immune cells. To distinguish whether the effect of cell proliferation or the immune system might be the major mechanism that accounts for the WSX1-dependent tumor growth inhibition *in vivo*, we tested tumor growth in wild-type, perforin (NK), and Rag (T, B) knockout mice.

Similar to wild-type mice, tumor growth reduction between TC1-GFP and TC1-WSX1 was found also in T and B knockout mice (Fig. 4*Aleft* vs. *middle*). However, the absence of perforin almost completely impaired the ability of WSX1 to inhibit tumor growth as there is no statistically significant difference in tumor growth between GFP and WSX1 tumors (Fig. 4*Aright*). This result suggests that WSX1 may sensitize NK cell surveillance for inhibiting WSX1 positive tumor growth. To further support this statement, tumors engineered with control GFP gene grew at a similar rate regardless of the presence or absence of NK or T cells (Fig. 4*B, left*). In contrast, WSX1-positive TC1 tumors disappeared in three out of four wild-type mice, grew very slowly in T and B deficient mice (reaching 50 $mm^3$ by day 40 after tumor inoculation), and developed aggressively in NK deficient mice (averaging 450 $mm^3$ by day 40, almost nine times higher than in T and B knockout mice) (Fig. 4*B*, *right*). To confirm that this observation was not dependent on a single clone, another independent clone (TC1-WSX1-

CL2) was tested *in vivo*. Similar to the other engineered WSX1 positive TC1 clone, TC1-WSX1-CL2 was eradicated in 4 out of 4 wild-type mice, while it reached 200 $mm^3$ by day 38 in NK deficient mice (Fig. 4*C*). These findings suggest that our observation is not clone-dependent.

Similar to the TC1 model, the WSX1-positive AT84 tumor cells grew slower than the control AT84-GFP in both the wild-type and T and B cell deficient mice (Fig. 4*Dleft vs. middle*). To test the WSX1-mediated NK cell dependence for the AT84 tumor model, STAT1 knockout mice were used because STAT1 is an essential transcription factor for NK cell function. In the absence of STAT1, these mice demonstrate impaired NK activity *in vitro* and fail to reject NK-sensitive tumors *in vivo* (12). As expected, no difference in the growth of control and WSX1-positive AT84 tumors was detected in these NK-defective STAT1 deficient mice (Fig. 4*Dright*).

## WSX1 suppression of tumor growth is independent of IL27

The presented results strongly suggest that WSX1 may play an antitumor role independent of IL27 since the endogenous level of IL27 is undetectable in mice. To exclusively confirm the role of IL27, since the cooperation among WSX1 expression in tumor cell and NK cell is needed for antitumor activity, and IL27 signals in both tumor and immune cells, WSX1-mediated tumor growth inhibition was compared in EBI3 knockout mice. Because EBI3 is a subunit of IL27, the lack of EBI3 would result in inhibition of IL27 signaling in both the host and tumor. As expected, lack of endogenous IL27 did not affect WSX1-mediated tumor growth suppression and a similar difference in tumor growth between TC1-GFP and TC1-WSX1 was found in wild-type mice as was found in IL27 EBI3 knockout mice (Fig. 4*Aleft* vs. 5*A*).

To further extend this exclusive confirmation, tumor growth in WSX1 knockout mice was also tested. Because WSX1 is a specific receptor for IL27, the lack of WSX1 in these mice should impede IL27 signaling in the immune cells. Similar to EBI3 knockout mice, WSX1-mediated tumor growth suppression was retained in WSX1 knockout mice (Fig. 5*B*). Moreover, WSX1 positive tumors grow at a similar rate in wild-type, EBI3, and WSX1 knockout mice (Fig. 5*C*). These results support our hypothesis that WSX1 retains its ability to impede tumor growth in the absence of IL27 signaling in either tumor or host cells.

## WSX1 sensitizes NK cell-surveillance by inducing NKG2D ligand expression in tumor cells

Our data above clearly demonstrate that the ability of WSX1 to suppress tumor growth is dependent on NK cells and independent of IL27 signaling in either the tumor or the host. The question is whether the presence of WSX1 in tumor cells directly sensitizes NK cell-mediated cytotoxicity. To accomplish this goal, NK cell cytotoxicity was compared between TC1-GFP and TC1-WSX1 cells. These assays revealed that TC1-WSX1 cells are more efficiently lysed when compared to the TC1-GFP cells (Fig. 6*Aleft*). To rule out the role of CD8 T cells, we used perforin and Rag knockout splenocytes. Similar to wild-type splenocytes (Fig. 6*Aleft*), splenocytes from Rag knockout mice lysed TC1-WSX1-positive cells more efficiently than TC1-GFP (Fig. 6*Amiddle*). Contrarily, the lack of perforin eliminated the enhanced cytolytic activity against TC1-WSX1 (Fig. 6*Aright*). Similarly, cytotoxicity against AT84-WSX1 was significantly higher than AT84-GFP (Fig. 6*B*). These results indicate that WSX1 expression in tumor cells provokes a direct NK cell surveillance.

One possible hypothesis is that WSX1 increases NK cell cytotoxicity by promoting the interaction between tumor cells and NK cells. Given that NKG2D is one of the primary receptors that promotes tumor cell surveillance (13), we determined whether the expression of WSX1 in tumors upregulates expression of NKG2D ligands. Flow cytometry analysis using an NKG2D/Fc binding assay (a reagent that detects cell-surface expression of all known

NKG2D ligands) confirmed the hypothesis that WSX1, but not GFP, greatly enhanced the expression of NKG2D ligands (Fig. 6*Cleft and middle*). Such ability of WSX1 to induce the expression of NKG2D ligands is more pronounced in the TC1 model than in the AT84 model (Fig. 6*Cright*).

To definitely confirm the hypothesis that upregulation of NKG2D ligands by WSX1 expression is the central mechanism to enhance NK-mediated cytolytic activity against WSX1 positive tumor cells, NKG2D receptors on NK cells were blocked using anti-mNKG2D C7 in the cytolytic assay (14). As expected, addition of an NKG2D neutralization antibody, anti-mNKG2D C7, substantially reduced NK cell lysis against both TC1-WSX1 and AT84-WSX1 target cells to levels comparable of GFP counterparts (Fig. 6*Dleft and middle*). Furthermore, WSX1 expression is strongly correlated ($R^2$= 0.7293) to MICA expression in human cancer cell lines (Fig. 6*Dright*).

## Discussion

Although it is well known that WSX1 is expressed in T and NK cells and is a critical receptor for triggering immune responses via IL27 signaling in these cells (1,2,15), our recent results revealed that WSX1 is also expressed in epithelial tumor cells such as breast tumor cell lines, while others have found its expression in human melanoma (3) and leukemia cells (16). Neither us nor others have quantified the level of WSX1 expression and compared the level of expression between epithelial tumor cells and normal epithelial cells. In this study, using a quantitative real-time PCR assay, we surprisingly found that WSX1 is not only expressed in most of the tested epithelial cells (8 out of 10), but is also expressed 13- to 78-fold higher than normal epithelial cells (Fig. 1 A).

While the function of WSX1 in immune cells has been studied extensively, its function in epithelial tumor cells has hardly been studied. In immune cells, it is generally accepted that IL27 possesses both pro- and anti-inflammatory properties (17–25). For example, IL27 induces key components to Th1 commitment such as synergistic induction of IFNγ with IL12, proliferation of naive $CD4^+$T cells, induction of T-bet and IL12Rβ expression, and possesses T-cell and NK cell mediated antitumor activities (15,20–25); however, parasitic studies show that the absence of WSX1 triggers aberrant cytokine production (26,27). In contrast to previous studies in immune cells, our findings assign a new role to WSX1 in epithelial cancer cell biology, that expression of WSX1 inhibits epithelial tumor growth *in vitro* and *in vivo* (Figs. 1,3, and 4). Such an observation was confirmed in two independent tumor models, TC1 and AT84. However, this observation is different in tumors derived from immune cells in which WSX1 elicited antiapoptotic and mitogenic signals (16) and transformed two leukemia cell lines, 32D and BaF3.

Different from the recent report in which WSX1 expression in epithelial melanoma cells requires IL27 to inhibit its tumor cell proliferation and tumor growth (3), our results provide a strong case of IL27-independent antitumor activity by WSX1 (Fig. 2 and 5). First, IL27 independence was demonstrated by our trial showing that WSX1 expression inhibited tumor growth in mice that lacked the IL27 subunit EBI3, the same as found in wild-type mice (Fig. 5 A). Second, WSX1 expression in epithelial tumor cells inhibits tumor growth in WSX1 knockout mice (Fig. 5 B).

Currently, no linkage between WSX1 expression in tumor cells and NK cell-mediated surveillance is reported in the literature. Using two different tumor models, TC1 and AT84, we show that WSX1 suppresses tumor growth *via* NK cells. In perforin and STAT1 knockout mice, WSX1-dependent suppression of tumor growth is impaired (Fig. 4), while *in vitro* WSX1 tumor cells are more sensitive to NK cell cytotoxicity (Fig. 6). Such phenomena are dependent

on the NKG2D pathway, as the presence of WSX1 directly enhances the expression of NKG2D ligands (Fig. 6) thereby enhancing NK cell-mediated recognition and release of cytotoxic molecules towards tumor cells.

Considering that WSX1 expression in our tumor models inhibits tumor growth while expression of WSX1 in certain leukemia cell lines confers transformation (16), further work is needed to investigate the molecular mechanism downstream of WSX1 that leads to opposing consequences between epithelial and blood-derived tumors. This link between WSX1 and NKG2D ligands, which are the intrinsic sensors of oncogenic transformation that induce innate immunosurveillance (28), suggests that WSX1 expression in epithelial tumor cells might play a role to prevent tumorigenesis but was eventually overridden by the defaulted pathway or immune escape mechanism. Such a scenario is also seen with the MICA-NKG2D surveillance system in which a high level of MICA expression in tumor cells were subjected to NKG2D surveillance (29,30), but this surveillance system was overridden by the aggressive tumors due to the development of multiple immune escape mechanisms (31,32). The connection of WSX1 to innate immunosurveillance could explain the observed discrepancy among the two tumor models used in this study: WSX1 is more effective in inhibiting tumor growth and increasing NKG2D ligand expression in TC1 model, a HPV-transformed normal cell line, than in aggressive AT84 models, a spontaneously arising oral squamous cell tumor of C3H mice, albeit WSX1 expression is higher in AT84 than in TC1.

In summary, this study exposed a novel function of WSX1 in epithelial tumor cells, linked WSX1 to NK-mediated antitumor immunosurveillance, and, most importantly, revealed that WSX1 induces an antitumor function by upregulating the expression of NKG2D ligands and this process is independent of the IL27 signaling pathway.

## Acknowledgments

**Financial Support**: This study was supported by NIH grant RO1CA120895 and NIH/NIBIB grant R21EB007208

We thank Dr. Fred de Sauvage for providing TCCR/WSX1 deficient mice.

## References

1. Chen Q, Ghilardi N, Wang H, et al. Development of Th1-type immune responses requires the type I cytokine receptor TCCR. Nature 2000;407:916–20. [PubMed: 11057672]
2. Pflanz S, Hibbert L, Mattson J, et al. WSX-1 and glycoprotein 130 constitute a signal-transducing receptor for IL-27. J Immunol 2004;172:2225–31. [PubMed: 14764690]
3. Yoshimoto T, Morishima N, Mizoguchi I, et al. Antiproliferative activity of IL-27 on melanoma. J Immunol 2008;180:6527–35. [PubMed: 18453571]
4. Worsham MJ, Chen KM, Tiwari N, et al. Fine-mapping loss of gene architecture at the CDKN2B (p15INK4b), CDKN2A (p14ARF, p16INK4a), and MTAP genes in head and neck squamous cell carcinoma. Arch Otolaryngol Head Neck Surg 2006;132:409–15. [PubMed: 16618910]
5. Lin KY, Guarnieri FG, Staveley-O'Carroll KF, et al. Treatment of established tumors with a novel vaccine that enhances major histocompatibility class II presentation of tumor antigen. Cancer Res 1996;56:21–6. [PubMed: 8548765]
6. Puisieux I, Odin L, Poujol D, et al. Canarypox virus-mediated interleukin 12 gene transfer into murine mammary adenocarcinoma induces tumor suppression and long-term antitumoral immunity. Hum Gene Ther 1998;9:2481–92. [PubMed: 9853515]
7. Liu L, Chahroudi A, Silvestri G, et al. Visualization and quantification of T cell-mediated cytotoxicity using cell-permeable fluorogenic caspase substrates. Nat Med 2002;8:185–9. [PubMed: 11821904]
8. Li S, Zhang L, Torrero M, Cannon M, Barret R. Administration route- and immune cell activation-dependent tumor eradication by IL12 electrotransfer. Mol Ther 2005;12:942–9. [PubMed: 15953768]

9. Bednarek AK, Keck-Waggoner CL, Daniel RL, et al. WWOX, the FRA16D gene, behaves as a suppressor of tumor growth. Cancer Res 2001;61:8068–73. [PubMed: 11719429]
10. Freedman VH, Shin SI. Cellular tumorigenicity in nude mice: correlation with cell growth in semi-solid medium. Cell 1974;3:355–9. [PubMed: 4442124]
11. Hoffman RM. In vitro sensitivity assays in cancer: a review, analysis, and prognosis. J Clin Lab Anal 1991;5:133–43. [PubMed: 2023059]
12. Lee CK, Rao DT, Gertner R, Gimeno R, Frey AB, Levy DE. Distinct requirements for IFNs and STAT1 in NK cell function. J Immunol 2000;165:3571–7. [PubMed: 11034357]
13. Hayakawa Y, Kelly JM, Westwood JA, et al. Cutting edge: tumor rejection mediated by NKG2D receptor-ligand interaction is dependent upon perforin. J Immunol 2002;169:5377–81. [PubMed: 12421908]
14. Ho EL, Carayannopoulos LN, Poursine-Laurent J, et al. Costimulation of multiple NK cell activation receptors by NKG2D. J Immunol 2002;169:3667–75. [PubMed: 12244159]
15. Pflanz S, Timans JC, Cheung J, et al. IL-27, a heterodimeric cytokine composed of EBI3 and p28 protein, induces proliferation of naive CD4(+) T cells. Immunity 2002;16:779–90. [PubMed: 12121660]
16. Pradhan A, Lambert QT, Reuther GW. Transformation of hematopoietic cells and activation of JAK2-V617F by IL-27R, a component of a heterodimeric type I cytokine receptor. Proceedings of the National Academy of Sciences of the United States of America 2007;104:18502–7. [PubMed: 18003935]
17. Bettelli E, Carrier Y, Gao W, et al. Reciprocal developmental pathways for the generation of pathogenic effector TH17 and regulatory T cells. Nature 2006;441:235–8. [PubMed: 16648838]
18. Batten M, Li J, Yi S, et al. Interleukin 27 limits autoimmune encephalomyelitis by suppressing the development of interleukin 17-producing T cells. Nat Immunol 2006;7:929–36. [PubMed: 16906167]
19. Awasthi A, Carrier Y, Peron JP, et al. A dominant function for interleukin 27 in generating interleukin 10-producing anti-inflammatory T cells. Nat Immunol 2007;8:1380–9. [PubMed: 17994022]
20. Chiyo M, Shimozato O, Yu L, et al. Expression of IL-27 in murine carcinoma cells produces antitumor effects and induces protective immunity in inoculated host animals. Int J Cancer 2005;115:437–42. [PubMed: 15688376]
21. Takeda A, Hamano S, Yamanaka A, et al. Cutting edge: role of IL-27/WSX-1 signaling for induction of T-bet through activation of STAT1 during initial Th1 commitment. J Immunol 2003;170:4886–90. [PubMed: 12734330]
22. Hisada M, Kamiya S, Fujita K, et al. Potent Antitumor Activity of Interleukin-27. Cancer Research 2004;64:1152–6. [PubMed: 14871851]
23. Morishima N, Owaki T, Asakawa M, Kamiya S, Mizuguchi J, Yoshimoto T. Augmentation of Effector $CD8^+$ T Cell Generation with Enhanced Granzyme B Expression by IL-27. The Journal of Immunology 2005;175:1686–93. [PubMed: 16034109]
24. Oniki S, Nagai H, Horikawa T, et al. Interleukin-23 and Interleukin-27 Exert Quite Different Antitumor and Vaccine Effects on Poorly Immunogenic Melanoma. Cancer Research 2006;66:6395–404. [PubMed: 16778218]
25. Salcedo R, Stauffer JK, Lincoln E, et al. IL-27 mediates complete regression of orthotopic primary and metastatic murine neuroblastoma tumors: role for CD8+ T cells. J Immunol 2004;173:7170–82. [PubMed: 15585838]
26. Artis D, Villarino A, Silverman M, et al. The IL-27 Receptor (WSX-1) Is an Inhibitor of Innate and Adaptive Elements of Type 2 Immunity. The Journal of Immunology 2004;173:5626–34. [PubMed: 15494513]
27. Villarino A, Hibbert L, Lieberman L, et al. The IL-27R (WSX-1) is required to suppress T cell hyperactivity during infection. Immunity 2003;19:645–55. [PubMed: 14614852]
28. Unni AM, Bondar T, Medzhitov R. Intrinsic sensor of oncogenic transformation induces a signal for innate immunosurveillance. Proceedings of the National Academy of Sciences of the United States of America 2008;105:1686–91. [PubMed: 18223157]
29. Raulet DH. Roles of the NKG2D immunoreceptor and its ligands. Nature reviews 2003;3:781–90.
30. Pende D, Rivera P, Marcenaro S, et al. Major histocompatibility complex class I-related chain A and UL16-binding protein expression on tumor cell lines of different histotypes: analysis of tumor

susceptibility to NKG2D-dependent natural killer cell cytotoxicity. Cancer Res 2002;62:6178–86. [PubMed: 12414645]

31. Zwirner NW, Fuertes MB, Girart MV, Domaica CI, Rossi LE. Cytokine-driven regulation of NK cell functions in tumor immunity: role of the MICA-NKG2D system. Cytokine Growth Factor Rev 2007;18:159–70. [PubMed: 17324607]
32. Rabinovich GA, Gabrilovich D, Sotomayor EM. Immunosuppressive strategies that are mediated by tumor cells. Annu Rev Immunol 2007;25:267–96. [PubMed: 17134371]

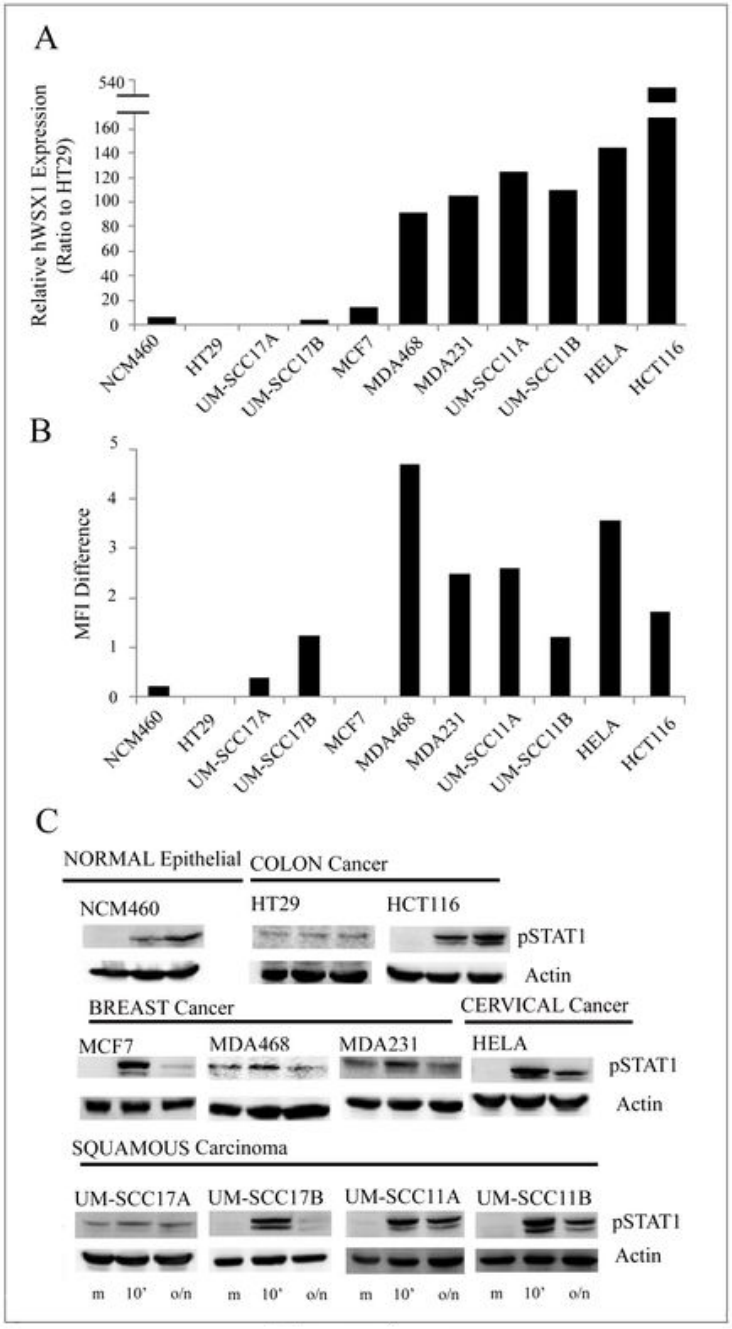


**Figure 1. Quantitative and functional analysis of WSX1 in a variety of human epithelial cell lines**

*A*, determination of the level of WSX1 expression using Quantitative Real-time PCR. The levels of WSX1 mRNA are normalized to actin mRNA, and the data shown is the relative expression of each cell line to HT29. *B*, detection of WSX1 expression at the protein level via flow cytometry. Cells were stained with the isotype control or with anti-human WSX1 antibody followed by anti-mouse-PE and median fluorescence intensity (MFI) difference was calculated as difference in MFI between isotype control and WSX1-stained cells. *C*, detection of functional WSX1 in tumor cells. Cells were treated with IL27 for 10 min (10′), overnight (o/n), or left untreated (m). Cell extracts were analyzed using western blot technique and probed with anti-pSTAT1 and actin antibodies.

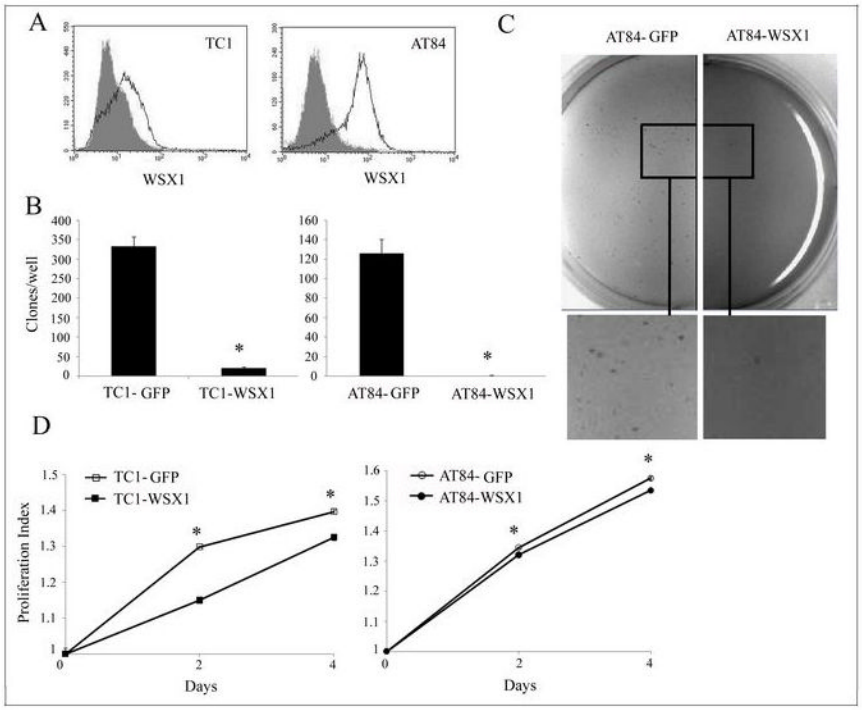


**Figure 2. WSX1 reduces tumorigenecity and proliferation of epithelial tumor cells**

*A*, detection of WSX1 expression in TC1 and AT84 tumor cells with flow cytometry. TC1 and AT84 tumor cells were transduced with retroviruses containing either control GFP (gray) or WSX1 gene (not shaded). The established stable cell lines were stained with a monoclonal WSX1 antibody followed by an anti-hamster-PE antibody. The data is representative of two independent clones. *B*, comparative analysis of soft agar growth assay between GFP and WSX1 in two different cell lines, TC1 and AT84. The data is representative of two independent clones, each performed in triplicate. *C*, a low-magnification photograph of clones formed of AT84-GFP vs. AT84-WSX1. *D*, GFP and WSX1 positive TC1 and AT84 cells were harvested on indicated days and analyzed for ATP release N=4. Error bars are smaller than symbols. *Columns*, mean; *bars*, SD *, $P < 0.05$

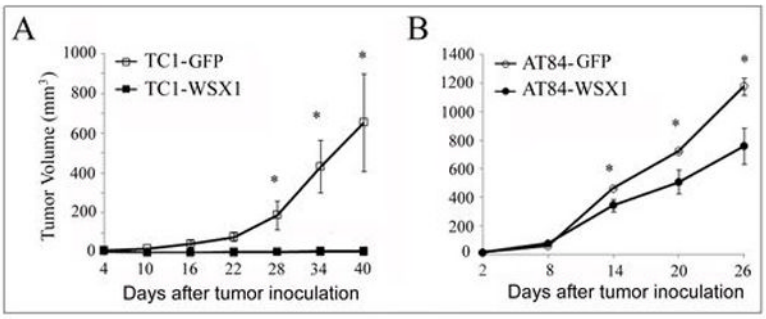


**Figure 3. WSX1 suppresses tumor growth *in vivo* in both TC1 and AT84 tumor models**

*A*, comparison of tumor growth between TC1-GFP and TC1-WSX1 in C57Bl/6 mice. *B*, comparison of tumor growth between AT84-GFP and AT84-WSX1 in C3H mice, N=4–5. *Points*, mean; *bars*, SD. *, $P < 0.05$.

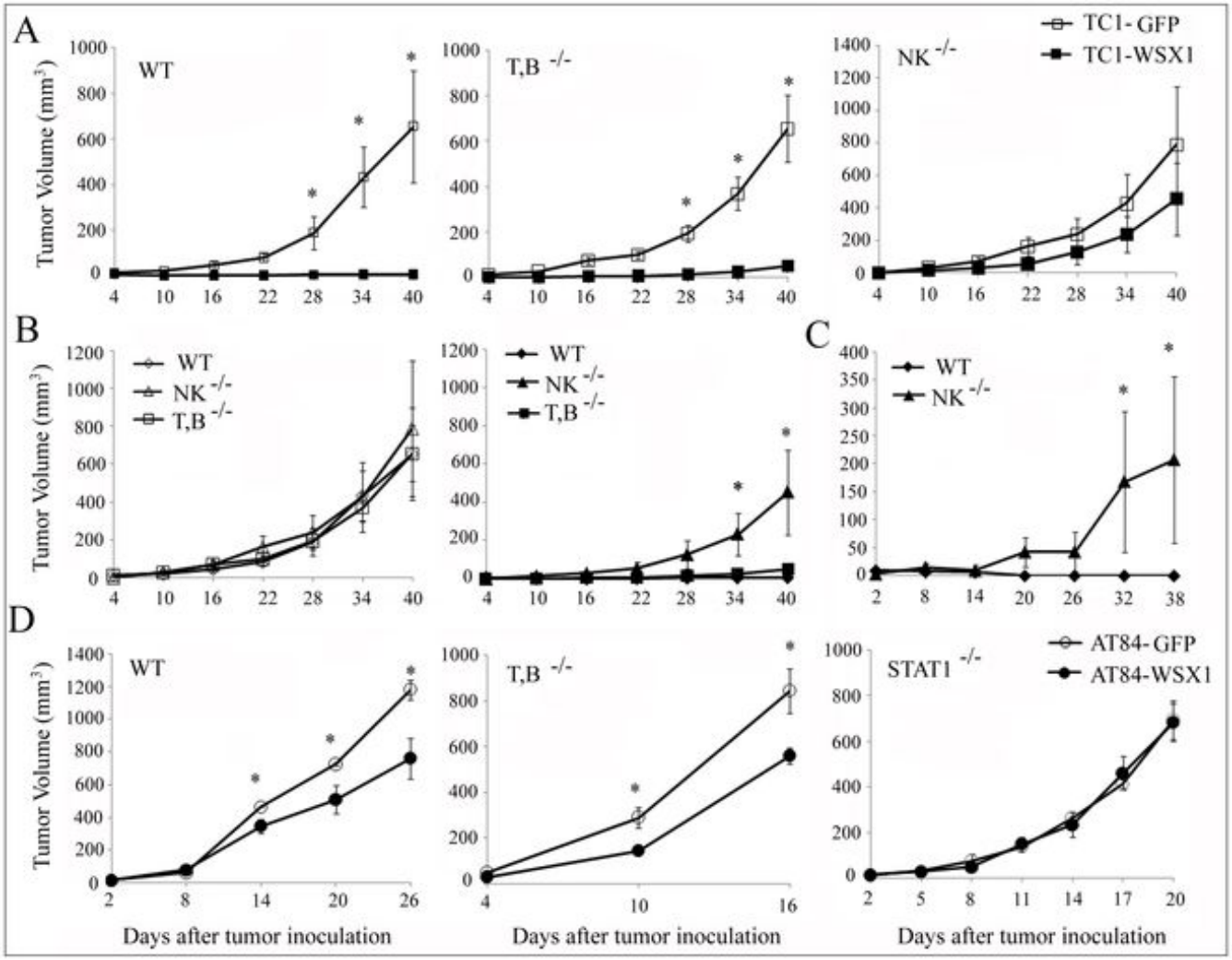


**Figure 4. WSX1-mediated suppression of tumor growth is dependent on NK cells**

*A*, comparison of tumor growth between TC1-GFP and TC1-WSX1 in C57Bl/6 wild-type (WT) mice (*left*), Rag ($T,B^{-/-}$) (*middle*), and perforin ($NK^{-/-}$) knockout mice (*right*). *B*, differential display of tumor growth rate of TC1-GFP (*left*) or TC1-WSX1 (*right*) in different immune knockout models such as C57Bl/6 wild-type (WT), Rag ($T,B^{-/-}$), and perforin ($NK^{-/-}$) knockout mice. *C*, comparison of tumor growth in C57Bl/6 wild-type (WT) mice and perforin knockout ($NK^{-/-}$) mice for an independent clone of TC1-WSX1 (TC1-WSX1 CL2). *D*, comparison of tumor growth between AT84-GFP and AT84-WSX1 in C3H wild-type (WT) (*left*), SCID ($T,B^{-/-}$) (*middle*), and STAT1 ($STAT1^{-/-}$) knockout mice (*right*), N=3–5. *Points*, mean; *bars*, SD. *, $P < 0.05$.

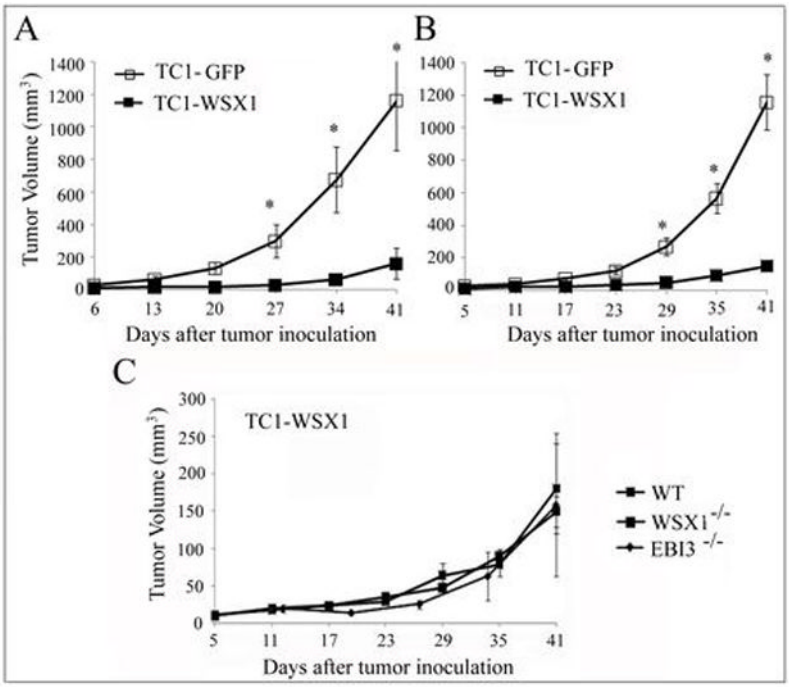


**Figure 5. WSX1 suppression of tumor growth is independent of IL27**

*A* and *B*, Comparison of tumor growth between TC1-GFP and TC1-WSX1 in (*A*) EBI3 knockout (EBI3$^{-/-}$) and (*B*) WSX1 knockout (WSX1 $^{-/-}$) mice. *C*, comparison of TC1-WSX1 tumor growth in C57Bl/6 (WT), WSX1$^{-/-}$, and EBI3$^{-/-}$ mice, N= 4–5. *Points*, mean; *bars*, SD. *, $P < 0.05$.

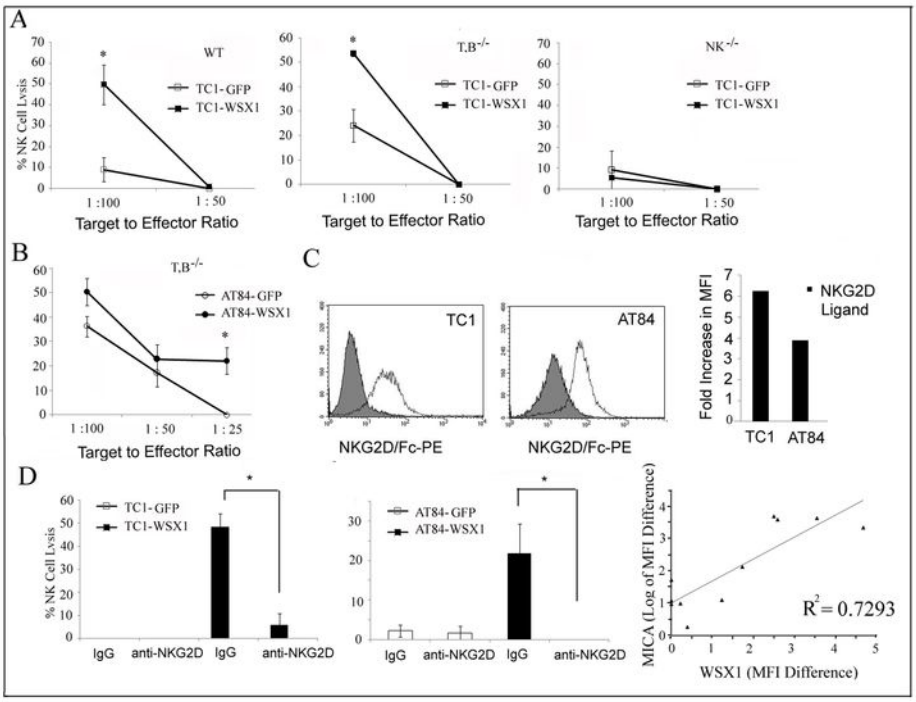


**Figure 6. WSX1 sensitizes NK cell lysis *in vitro* via an NKG2D pathway**

*A*, NK cell activity against TC1-GFP and TC1-WSX1 was analyzed from lymphocytes derived from (*A)* C57Bl/6 wild-type (WT) mice (*left*), Rag ($T,B^{-/-}$) (*middle*), and perforin ($NK^{-/-}$) knockout mice (*right*). Viable target cells from triplicate wells were counted using a fluorescence microscope. *B*, NK cell activity against AT84-GFP vs. AT84-WSX1 was analyzed from lymphocytes derived from SCID mice ($T,B^{-/-}$). The graphs represent data from three independent experiments. *C*, comparison of NKG2D ligands expression in TC1 (*left*) and AT84 (*middle*) tumor cells transduced with GFP (gray) or WSX1 gene (not shaded). The indicated cells were stained with NKG2D/Fc followed by anti-human IgG-PE and fold induction in MFI was calculated between each pair (*right*). *D*, NK cell activity in the presence of anti-NKG2D antibody or isotype control against TC1-GFP and TC1-WSX1 (*left*) at 1:100 target to effector ratio, or AT84-GFP and AT84-WSX1 *(middle*) at 1:25 target to effector ratio. Correlation of WSX1 and MICA expression in the human tumor cells indicated in Fig 1. Cells were stained with the isotype control, WSX1, or MICA and MFI difference between isotype and WSX1 or MICA antibody was plotted (*right*). The plotted values of MFI for MICA expression were log-transformed. *Points*, mean; *bars*, SD. *, $P < 0.05$.